



Seismic failure probability evaluation of FBR equipment on an isolated plant

Sekiya H.⁽¹⁾, Kamishima Y.⁽²⁾, Tanaka K.⁽³⁾

(1) Mitsubishi Heavy Industries, Japan

(2) Advanced Reactor Technology Company, LTD, Japan

(3) Tokyo Electric Power Company, Japan

ABSTRACT : A fragility assessment based on safety factors was carried out for major equipment in a base-isolated Fast Breeder Reactor (FBR) plant.

The authors propose a method for evaluating the non-linear response factor of an isolated building and the capacity factor of the equipment subjected to the modified seismic accelerations. The results show that the hardening point of the isolation devices ,i.e., the skeleton of the rubber bearings is dominant in the failure probability and the shape of the fragility curve.

1. INTRODUCTION

In the design of a FBR, the application of a seismic isolation system is effective for reducing the seismic loads which are critical to the structural design of equipment. [1] From the safety point of view, however, the impact of the application on overall plant safety should be examined using quantitative methods such as a seismic probabilistic safety assessment (PSA). In the seismic PSA the failure probabilities of equipment are calculated as a function of input acceleration.

Although a base-isolated building responds almost linearly for design level inputs, the response shows a non-linear tendency after the isolation system i.e. the rubber bearings are displaced beyond a hardening point. Therefore particular consideration should be given to dealing with this non-linearity since the previous safety factor method has been based on the assumption that the building will respond linearly.

In this study, a fragility assessment based on response and capacity factors was carried out for the reactor vessel (RV) taking account of the non-linearity of the isolation system.

2. DESIGN DESCRIPTION

2.1 Base-isolated building

The FBR plant is base-isolated in the horizontal direction. [1] The isolation system is composed of natural rubber bearings and steel dampers. The design specification of the base-isolation system is as follows:

Horizontal	Initial period T_1	1.0 sec	
	Isolated period T_2	2.0 sec	
	Yield coefficient	0.05	
Vertical	Natural period	0.05 sec	
	Supporting load	750 ton	(per rubber bearing)
Rupture displacement		68.9 cm	
Displacement for S_2 earthquake		14.0 cm	

2.2 Reactor vessel

The RV is installed at the level in the base-isolated building shown in Fig. 1. The RV has a diameter of 10.4 m and a thickness of 35 mm. Its natural frequency for a single degree of freedom is 5 Hz horizontally and 11.6 Hz vertically. The effective mass W is 2000 ton and the damping factor is 0.01. The stress on the RV σ_{RV} induced by the seismic loads can be expressed by:

$$\sigma_{RV} = \sigma_b + \sigma_m = \frac{M}{Z} + \frac{F}{A} \quad (1)$$

where M : Bending moment = $L_m \times W \times \alpha_H$ (horizontal acceleration)
 F : Axial force = $W \times \alpha_V$ (vertical acceleration)

3. OUTLINE OF FRAGILITY ANALYSIS

The fragility, e.g., the conditional frequency of failure P_f for a given peak ground acceleration (PGA) level, a , is generally given by three constants, i.e., median ground acceleration A and logarithmic standards β_R and β_U [2]:

$$P_f = \Phi \left[\frac{\ln\left(\frac{a}{\check{A}}\right) + \beta_U \Phi^{-1}(Q)}{\beta_R} \right] \quad (2)$$

where $\check{A} = F \times A_{S_2}$
 Φ : Standard Gaussian cumulative distribution function

The particular features of the fragility analysis are as follows:

- (1) The non-linear response factor is defined as a function of PGA, a .
- (2) Consequently the safety factor F and \check{A} ($= F \times S_2$) become functions of PGA, a .
- (3) The uncertainty of the response caused by the variabilities in the building and isolation system are calculated at several input levels. However an enveloped value is applied to the response factor for simplicity and conservatism.
- (4) The spectral shape of the input motion is assumed to be the design earthquake S_2 .
- (5) Buckling is considered as the failure mode of the RV.

4. RESPONSE ANALYSIS OF THE ISOLATED BUILDING

4.1 Non-linearity characteristics

(1) Objectives

Analyses were made to evaluate the tendency to non-linearity in the response of the base-isolated building and its impact on the response of the RV.

(2) Analytical condition

The analytical model of the isolated building is shown in Fig. 1. The model is a single-stick lumped mass model which both the isolation layer and the soil-structure interaction are considered as springs. The effect of slippage of the rubber bearings was also considered. The design earthquake (S_2) has a peak acceleration of 0.388 G. Vertical motion is assumed to be 0.6 times the horizontal motion. By amplifying the input motion, the response of the isolated building were analyzed for the several input levels between S_2 and $3.5 \times S_2$.

(3) Analysis results

Fig. 2 shows the floor response spectra (FRS) at the level where the RV is installed. The horizontal FRS for higher inputs (over $2 \times S_2$) show low-period peaks due to the non-linearity of the isolation system. This is because the displacement of the rubber bearings exceeds their linear range.

Fig. 3 shows the acceleration of the floor at the level of RV. Fig. 4 shows the displacement and shear force of the isolation system. It is clear that the building responds linearly until the input increases to 2 times the S_2 earthquake, however its response increase drastically once the isolation system is displaced beyond the limit of linearity, i.e., the hardening point.

4.2 Uncertainty of responses

(1) Objectives

Analyses were made to evaluate the uncertainty in the responses of the base-isolated building based on a two-point estimation method.

(2) Analytical condition

The uncertainty of the responses were evaluated at S_2 , $2.5 \times S_2$, $3 \times S_2$. The variability in the soil springs, rubber bearings, steel dampers and skeleton of the concrete were considered to evaluate the uncertainty of the responses. (Fig. 1)

(3) Analysis results

Fig. 5 shows the COV of the FRS at RV equipped level. The level of COV increases as the input level increase because of the nonlinear response of the building. The COV is however less than 0.3 at these input levels and for the range of periods close to the RV natural frequency.

5. FRAGILITY ANALYSIS OF THE REACTOR VESSEL

5.1 Response factors

(1) Spectral factor F_{SA}

This factor represents the variability in the input motion and the associated ground response spectra. As mentioned in 3.1 (3), a uniform hazard spectrum is assumed to be same as the S_2 spectrum. Therefore $F_{SA}=1.0$ and $\beta_R=0.3$ for the response variability due to the variability in the input motion.

(2) Non-linear response factor F_{NL}

This factor represents the nonlinear response of the base-isolated building. Fig. 6 shows the normalized stress on the RV K_{NL} . The value of more than 1.0 for the large input level over 2 times S_2 implies a non-linear response of the base-isolated building. Thus F_{NL} was estimated to be $1/K_{NL}$ and $\beta_U=0.1$ for the uncertainty of the non-linearity.

(3) Spectral shape factor F_{SS}

This factor represents the uncertainties in the FRS caused by the variability in the base-isolated building. The 10% broadened FRS is used in the aseismic design of the RV. Therefore F_{SS} is defined by:

$$F_{SS} = \frac{(RV \text{ stress due to } 10\% \text{ broadened FRS})}{(RV \text{ stress due to actual FRS})} = 1.27$$

As mentioned in 4.2, the FRS has the variability shown in Fig. 5 and its COV is less than 0.3 for all input levels.

Therefore the enveloped value of 0.3 was used for β_R for simplicity although it overestimates the probability of RV failure at low input levels (e.g. $1.0 \times S_2$).

(4) Earthquake direction factor F_{EC}

This factor represents the earthquake component combination. The maximum stresses induced by horizontal and vertical forces are added in the design. It was assumed that the actual stress was the value estimated by SRSS and the summated value was a 95% confidence value. Therefore the factor is given by:

$$F_{EC} = \frac{(M/Z + F/A)}{\sqrt{(M/Z)^2 + (F/A)^2}}$$

The factor changes according to the input level since the ratio of the stresses depends on the input level. (See Table 1)

5.2 Capacity factors

(1) Strength factor F_s

This factor represents the ratio of the ultimate strength to the stress calculated in the design. The allowable stress σ_L in the design using the design yield stress and a factor of safety (F.S.) of 1.3 was 7.33 Kg/mm^2 . Therefore the medium buckling strength σ_m was given by:

$$\sigma_m = \frac{\sigma_{y,mean}}{\sigma_{y,min}} \times F.S. = 1.3 \times 1.5 \times 7.33 = 14.3 \text{ Kg/mm}^2$$

On the other hand, the design stress is 4.9 Kg/mm^2 . Therefore F_s was given by:

$$F_s = \frac{14.3}{4.9} = 2.92$$

Assuming $\sigma_{y,min}$ to be the 95% confidence value for $\sigma_{y,mean}$, β_R was given by:

$$\beta_R = \frac{\ln 1.3}{1.64} = 0.16$$

(2) Inelastic energy absorption factor F_μ

This factor represents the deamplification effect resulting from the inelastic energy absorption. Under repeated seismic loads, the nonlinear deformation produces a large damping effect in the seismic response. [3] Fig. 7 shows the actual seismic response including the damping is much less than the linear seismic response. The ratio $\bar{X}_\sigma / \bar{X}_e$ depends on the FRS at the RV floor level. In the $3.5 \times S_2$ case, the ratio was calculated by RV nonlinear analyses and the ratio was estimated to be 2.0. Therefore $F_\mu = 2.0$ and for the uncertainty in the RV nonlinear analyses.

5.3 Results

Table 2 summarizes the estimated safety factors. The safety factor F depends on the input level so that the medium ground acceleration capacity A changes as the input level increases. From the tendency shown in Fig. 4, the response of the RV was expected to increase drastically due to the hardening of the rubber bearings. Therefore F at $4 \times S_2$ was estimated to be 0.0 and was interpolated for a given PGA.

By substituting the values in the Eq. (2), the fragility curve shown in Fig. 8 was obtained.

5.4 Effects of the capacity of the RV and the isolation system on the fragilities

The following fragility analyses were made to evaluate the effect of the capacity of the RV and isolation system on the fragilities:

- a. RV wall thickness: 35 mm increased to 50 mm
- b. Rubber bearings: 750 ton decreased to 500 ton
(Rupture displacement : 68.9 cm increased to 103.4 cm)

The 95% confidence fragility curves are compared in Fig. 9. HCLPFs (High-Confidence, Low-Probability-of-Failure) and medium ground acceleration capacity in each case are summarized in Table 2.

6. DISCUSSION

The RV fragility has a sharply increasing shape because of the drastic increase in the RV response due to the hardening of the rubber bearings. From the curve for 95% non-exceedance probability, the HCLPF for RV buckling failure was estimated to be $2.6 \times S_2$ which implies sufficient seismic margin.

Comparing case 1 & 2, 3&4, HCLPF were increased to some extent ($2.6 \times S_2$ to $3.1 \times S_2$) due to increasing the wall thickness of RV. However, A shows only a small change because the increased capacity is cancelled out by the drastic increase in the response of the RV due to hardening. On the other hand, comparing case 1 & 3, 2&4, A was increased to some extent ($3.7 \times S_2$ to $4.2 \times S_2$) due to improving the capacity of the rubber bearings although the HCLPF shows a small change. Therefore it was concluded that the equipment fragilities in an isolated plant strongly depend on the hardening characteristics of the isolation system, i.e., the skeleton of the rubber bearings.

In other word, capacity of the equipment in a base-isolated building is generally between the initiation of the hardening and the rupture point of the rubber bearings irrespective of the strength of the equipment.

7. CONCLUSION

A fragility assessment based on response and capacity factors was carried out for a reactor vessel (RV) taking the non-linearity of the isolation system into account. The result shows that the skeleton of the rubber bearings is dominant in the failure probability and the shape of fragility curve irrespective of the strength of the equipment.

8. ACKNOWLEDGMENT

This study was carried out as a research project of Tokyo Electric Power Company, entitled "Seismic PSA for an FBR plant".

REFERENCES

1. Kato, M., Watanabe, Y., et al. 1995. Design study of the seismic-isolated reactor building of demonstration FBR plant in Japan. SMiRT-13, Vol.III: 579-584
2. R.P. KENNEDY and M.K. RAVINDRA 1984. Seismic fragilities for nuclear power plant risk studies. Nuclear Engineering and Design 79:47-68
3. Kawamoto, Y., Sasaki, N., et al. Reduction of Seismic Responses of Shell Structures with Nonlinear Deformation Characteristics. SMiRT-11, Vol.E:257-262

Table 1 Safety factors for RV Buckling (Case: RV: 35 mm Rubber bearing:750 ton)

Safety Factor	Input level					β_R	β_U	
	S_2	$2.25 \times S_2$	$2.75 \times S_2$	$3.5 \times S_2$	$4.0 \times S_2$			
F_S	2.92					0.16	0.1	Stress margin for the ultimate strength
F_μ	2.0					0.0	0.1	Inelastic energy absorption by RV
F_C	5.84					0.16	0.14	
F_{SS}	1.27					0.3	0.0	Uncertainty in FRS
F_D	1.0					0.0	0.1	Damping in RV
F_{SM}	1.0					0.0	0.1	Modeling of RV
F_{MC}	1.0					0.0	0.1	Modal combination
F_{EC}	1.22	1.30	1.35	1.39		0.2	0	Earthquake components
F_{ER}	1.55	1.65	1.71	1.77		0.36	0.17	
F_{SA}	1.0					0.3	0.0	Spectral shape of the input motion
F_M	1.0					0.0	0.1	Modeling of the building
F_{NL}	1.0	0.96	0.92	0.57	0	0.0	0.1	Nonlinearity of the building response
F_{SR}	1.0	0.96	0.92	0.57		0.3	0.14	
F^{*1}	9.05	9.25	9.19	5.89	0 ^{*2}	0.50	0.26	

*1 Interpolated values were computed at given input levels between the calculated input levels.

*2 $F=0.0$ at $4 \times S_2$ due to the drastic increase in the RV response before the rupture of the rubber bearings.

Table 2 Effects of changing RV strength and capacity of rubber bearings

Case	RV	Rubber bearing	HCLPF	A
1	35	750	2.6	3.7
2	50	750	3.1	3.8
3	35	500	2.6	4.2
4	50	500	3.5	4.3
	(mm)	(ton)	($\times S_2$)	($\times S_2$)

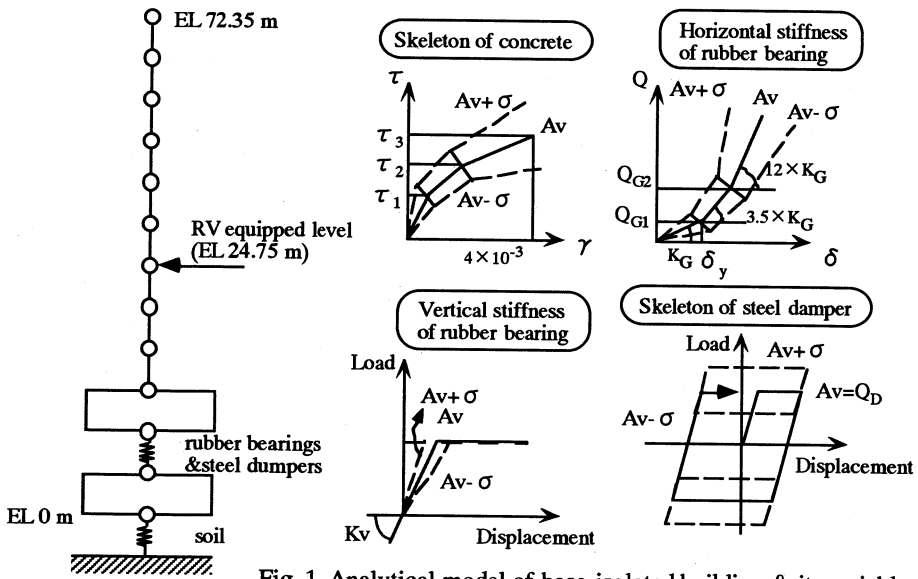


Fig. 1 Analytical model of base-isolated building & its variables

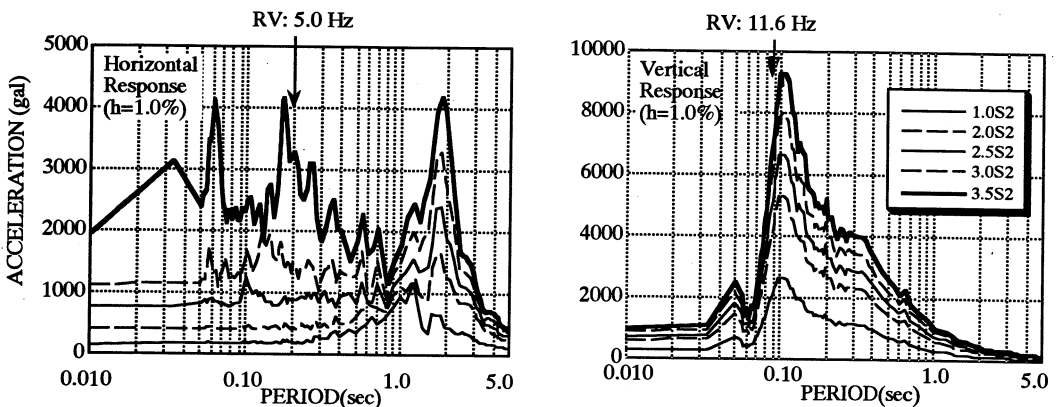


Fig. 2 Floor Response Spectra for various input levels

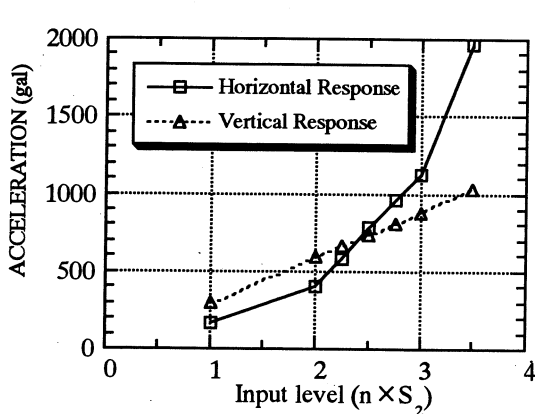


Fig. 3 Building response v.s. Input level

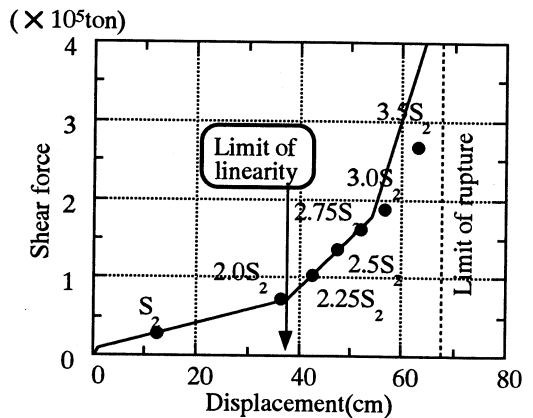


Fig. 4 Response of Isolation system v.s. Input level

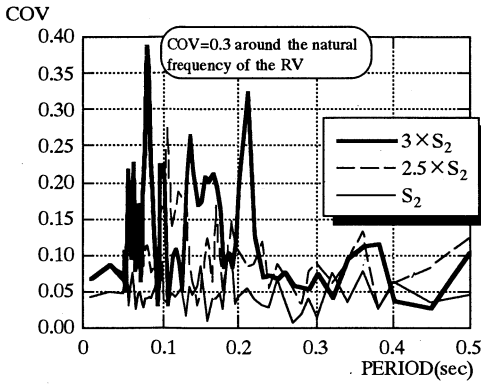


Fig.5 Response uncertainties due to the variability of the building

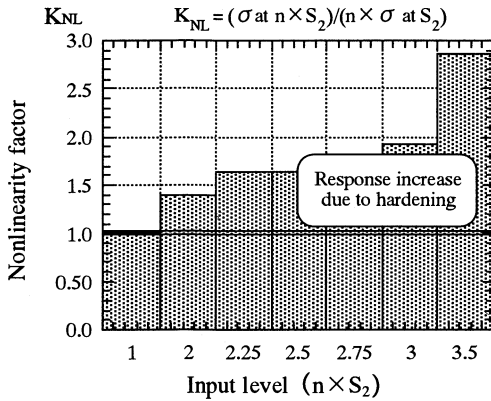


Fig. 6 Nonlinearity factor v.s. Input level

A: Critical point from linear calculation
 B: Actual critical point
 C: Ultimate limit state

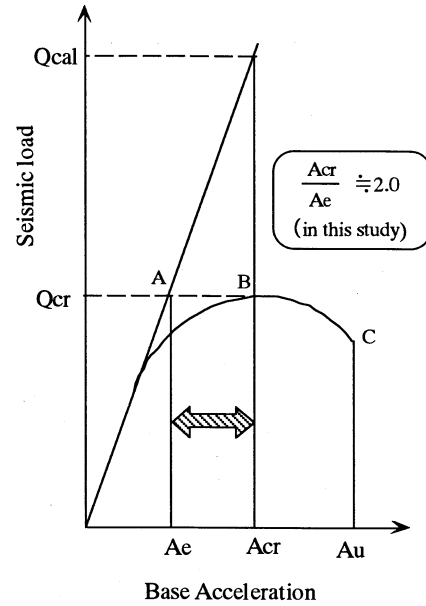


Fig. 7 Basic behavior of elasto-plastic buckling under seismic loads

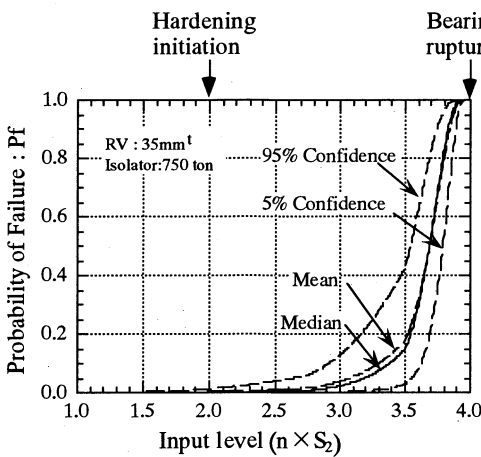


Fig.8 Fragility curve for RV buckling

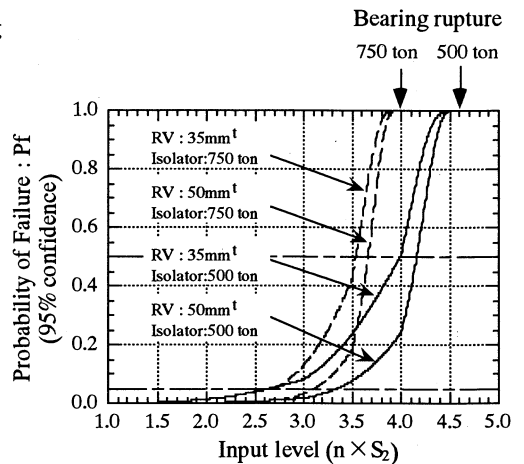


Fig.9 Effects of changing RV strength and capacity of rubber bearings